High-throughput study of the effects of inorganic additives and poisons on NH₃-SCR catalysts—Part I: V₂O₅–WO₃/TiO₂ catalysts

M. Klimczak, P. Kern, T. Heinzelmann, M. Lucas, P. Claus *

Department of Chemistry, Ernst-Berl-Institute/Chemical Technology II, Darmstadt University of Technology, Petersenstr. 20, D-64287 Darmstadt, Germany

ABSTRACT

The influence of phosphorus, alkaline and alkaline earth metals, chromium and copper on the catalytic activity and selectivity of a V₂O₅–WO₃/TiO₂ catalyst for the selective catalytic reduction (SCR) of nitrogen oxides with ammonia has been studied. These components are put through a catalytic aftertreatment system of a diesel engine as impurities of biodiesel (K, Na, P), urea solution (K, Na, Ca, Mg) and abrasion of the engine (Cr, Cu). The catalysts were exposed to corresponding nitrates or ammonium compounds in diluted solution by wet impregnation or deposition of inorganic aerosol particles. The second approach allows a more realistic investigation using catalysts and reaction conditions close to mobile application. Hereby, the effects of single catalyst poisons have been investigated. Furthermore, the influence of combinations of poisons using Design of Experiments (DOE) has been determined in case of impregnated catalysts. Physical and chemical characterization methods focusing on NH₃-TPD, penetration profiles and chemical analysis have been carried out to gain insight into the extent and the mechanism of deactivation. Both impregnated and aerosol deactivated catalysts show a strong poisoning effect of alkaline metals due to a reduced ammonia adsorption capacity. This effect could be weakened by a simultaneous doping of phosphates or sulphates. Chromium and copper are moderate catalyst poisons but have the ability to increase the N₂O production.

© 2009 Elsevier B.V. All rights reserved.

1. Introduction

Nitrogen oxides in exhaust gases from combustion of fossil fuels and biofuels are a main source for air pollution. High levels of NO_x lead to environmental damages, caused by acid rain and ozone depletion. Furthermore, they contribute to photochemical smog which contains poisons like ozone and peroxyacylnitrate. These environmental problems have resulted in a continuous decrease of the allowed NO_x concentrations due to stringent emission regulations.

The current technology for removal of nitrogen oxides in power plant emissions is the selective catalytic reduction with ammonia (NH₃-SCR) [1,2]. This catalytic aftertreatment system is also considered as the technology with the highest potential to meet strict future diesel emissions standards in mobile applications.

The catalyst for NH₃-SCR, optimized for diesel mobile application, contains 1.5–2.0 wt.% of V₂O₅ and ∼8 wt.% WO₃ on TiO₂ support. WO₃ is a promoter, which stabilizes the anatase modification of titania, increases the surface acidity of the catalyst and improves the resistance towards alkali metals [3]. Although a lot of studies have been carried out to explain the mechanistic aspects of

the SCR reaction a complete understanding has not been achieved. The form of bonded ammonia on the catalytic surface is still unclear even though these studies showed a common reaction of gaseous NO with adsorbed NH₃ through a Rideal-Eley mechanism. For a long time, a widely accepted mechanism of the SCR reaction was being proposed by Topsøe et al. [4]. It involves the adsorption of ammonia on Brønsted acid sites (V–OH), its activation by vanadyl groups (V=O) and a reaction with gaseous or weakly bonded NO. Density functional theory (DFT) calculations show an interaction of ammonia with Brønsted acid sites and a reaction with NO to form an adsorbed NH₂NO species which decomposes to N₂, H₂O and a reduced vanadium oxide cluster [5,6].

A major problem in practical applications of SCR catalysts has been their deactivation by different components in the exhaust gas, which accumulate on the catalyst surface. The origins of these poisons are, for instance, inorganic fuel oil additives, biodiesel impurities, lubricant oil additives and abrasion of the engine. Poisoning by various inorganic components has been investigated using different approaches for catalyst modification [7–17] like impregnation or exposure to aerosols. The main focus hereby was on the effect of phosphorus [7–10] and alkaline metals [10–17]. These components are of high interest because of their significant amount in biodiesel and lubricant oil additives. The poisoning effect of alkaline metals on the catalyst activity has been reported by several groups [10–17]. Chen and Yang [15] identified alkaline

* Corresponding author. Tel.: +49 6151 16 5369/4788; fax: +49 6151 16 4788.
E-mail address: claus@ct.chemie.tu-darmstadt.de (P. Claus).

metal oxides as very strong poisons, whereas the strength of the poisons increase with their basicity. The amount of ammonia adsorbed on Brønsted acid sites decreases with the amount of potassium deposited on the catalyst. The amount of ammonia bonded on Lewis sites is unaffected [15]. Phosphorus decreases the catalytic performance due to interactions with a catalyst component like stabilizing of inactive vanadium (4+) species [8] and pore blocking [8,9].

Furthermore, catalysts aged in mobile application and in power plants show deposits of different inorganic components resulting in a reduced catalyst activity [7,18–20]. The decreased catalytic performance has been the result of thermal and chemical deactivation by numerous components. Consequently, the identification of a single poison effect is therefore almost impossible. But significant deposits of calcium, phosphorus and zinc were found in aged catalysts [21,22].

In this work we investigated the effect of single poisons to V_2O_5–WO_3/TiO_2 catalysts. Different methods for catalyst doping, i.e. impregnation and poisoning by aerosols, were applied. Furthermore, multicomponent systems were used to screen for cumulative effects applying Design of Experiments (DOE). The effects of inorganic additives and poisons on Fe zeolites are presented in Part II.

2. Experimental

2.1. Catalysts

Ceramic honeycombs (Inocermic) with a cell density of 72 cpsi (200 channels) were used for high-throughput experiments. Catalysts with a cell density of 400 cpsi (7 × 7 channels) in a geometry of 150 mm × 10 mm × 10 mm were chosen for poisoning by aerosols. These monoliths were coated with an industrial V_2O_5–WO_3/TiO_2 powder, resulting in a powder content of 200 g/L. The different segments were calcined in air at 550 °C for 24 h prior to poisoning.

2.2. Deactivation of catalysts by impregnation and activity measurements

The monolithic honeycomb catalysts used for the high-throughput screening exhibit an uniform coating on the channel walls and are tight with respect to gas and liquid. Therefore, every single channel can be regarded as an individual plug-flow reactor which results in 128 individual reactors per a monolithic catalyst (remaining outer channels were used to fix the honeycomb during preparation and screening). Every channel was doped with inorganic components by an automated channel-by-channel impregnation procedure using a pipetting robot (Tecan Miniprep 60). The concentration of the precursor solution, removed after 5 s, resulted from the water adsorption capacity of the coating. The short impregnation time prevented that an active component was washed out and led to a reproducible preparation [23]. When the catalysts were dry they were calcined at 550 °C for 24 h. The described procedure was repeated after calcination in the case of immiscible combinations of catalyst poisons.

The SCR activity tests of every individual channel were conducted in an complex apparatus developed in our group. Main components of this high-throughput setup are a dosing/sampling- and a positioning system which allow a screening of every channel one after another. The gaseous feed of reactants was dosed through a concentrical annulus in a channel of the coated monolith and was then removed through a titanium capillary at a channel depth of 50 mm. A detailed description of this apparatus can be found elsewhere [23,24]. Typical feed gas composition was 1000 vppm NO, 1000 vppm NH₃, 1000 vppm CO, 5 vol.% CO₂, 8 vol.% O₂, 5 vol.% H₂O and, as balance, N₂. It was introduced consecutively to each channel, the remaining channels were kept under N₂ atmosphere. The experiments were carried out at temperatures of 250 °C, 350 °C and 450 °C and at a space velocity of 50,000 h⁻¹. Every channel was measured for 8 min which led to a total measurement time of approximately 20 h per monolithic honeycomb catalyst. Hereby, an effect of a long delay time between the first and the last measurement on the catalytic performance could be excluded. The reaction products were continuously analyzed by FTIR spectroscopy (Thermo Nicolet Antaris IGS). The volume of the gas cell was 200 mL so that a gas flow of 100 mL/min through this cell was applied.

2.3. Deactivation of catalysts by exposure to aerosols and activity measurements

400 cpsi honeycomb catalysts, obtained by cutting out of serial catalyst, were poisoned by aerosols at 500 °C and a space velocity of 50,000 h⁻¹ (95% air, 5% H₂O). The aerosols, which were generated by injecting diluted precursor solutions of catalyst poisons in the preheated zone, passed through three catalysts, which were placed parallel on this zone. This arrangement and a verification of air flows at the reactor exits make a defined and simultaneous poisoning of three different catalyst types (V_2O_5–WO_3/TiO_2, Fe zeolite, Pt/Al_2O_3 for NO oxidation) possible. A qualitative comparison of adhesion properties was also achieved. A description of the apparatus can be found elsewhere [24].

The activity of these catalysts was measured in a flow reactor at temperatures ranging from 200 °C to 450 °C and at a space velocity of 50,000 h⁻¹. The simulated exhaust gas consisted of 1000 vppm NO, 1000 vppm CO, 5 vol.% CO₂, 8 vol.% O₂, 5 vol.% H₂O, balance N₂ and NH₃ whereby the amount of ammonia varied stepwise between 200 vppm and 1200 vppm (α = NH₃,in/NOin = 0.2–1.2) at each temperature. Afterwards, deNOx activity at an ammonia slip of 25 vppm was determined by inter- or extrapolation. Furthermore, this measurement procedure allows an ammonia titration by interrupting the ammonia dosage of 1200 vppm. The analysis of the reactant products was carried out again with FTIR spectroscopy with a volumetric flow rate through the cell of 500 mL/min.

2.4. Characterization of fresh and deactivated catalysts

For the temperature-programmed desorption of ammonia (NH₃-TPD), V_2O_5–WO_3/TiO_2 powder has been applied. Catalyst poisons were introduced using incipent-wetness impregnation with nitrates of the corresponding metals or ammonium salts. NH₃-TPD measurements were conducted in a quartz-tube reactor with 0.5 g of catalyst powder because the washcoat could not be separated from the ceramic honeycomb. The calcined powder was dried at 200 °C (N₂, 450 mL/min). After cooling down to 50 °C the sample was saturated with ammonia for 15 min (2 vol.% NH₃, N₂). Physically adsorbed ammonia was removed in N₂ at a temperature of 150 °C. Desorption of chemisorbed ammonia was accomplished by heating the sample to a temperature of 525 °C with a ramp of 10 K/min in a N₂ flow of 450 mL/min. Ammonia storage capacities were obtained by integrating the FTIR signal.

Analyses of the specific surface area and texture (i.e., pore volume and pore size distribution) were carried out by N₂ physisorption using an Autosorb 3B (Quantachrome) instrument. The samples were dried at 150 °C for 24 h in vacuum prior to measurements. The specific surface area was calculated according to the BET method.

Chemical analysis of the catalysts with respect to the concentration of catalyst poisons was conducted with ICP-OES (inductively coupled plasma-optical emission spectrometry) or XRF (X-ray fluorescence).
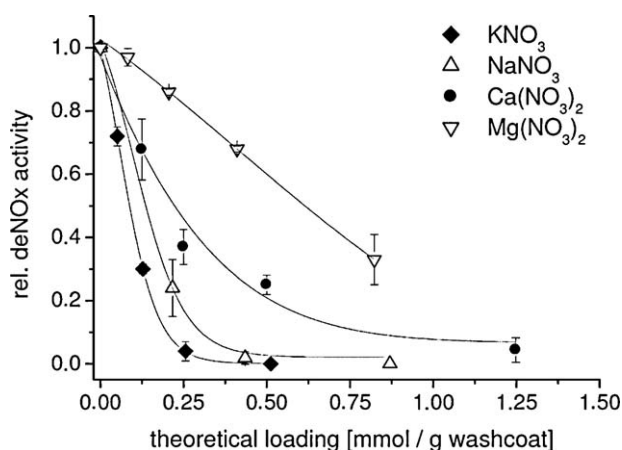
Fig. 1. Relative deNOx activity as a function of K, Na, Ca and Mg loading; conditions: 1000 vppm NO, 1000 vppm NH$_3$, 1000 vppm CO, 5 vol.% CO$_2$, 8 vol.% O$_2$, 5 vol.% H$_2$O and balance N$_2$ at 350 °C and 50,000 h^{-1}; poisoning of 72 cpsi monoliths by impregnation.

Fig. 3. NH$_3$-TPD curve of a fresh and K, Na, Ca and Mg poisoned catalysts. NH$_3$ adsorption temperature: 50 °C, temperature ramp: 10 K/min; poisoning of powders by impregnation.

The distribution and penetration depth of the additives was recorded by a combination of raster electron microscopy and energy-dispersive X-ray measurements (REM/EDX) by means of a Zeiss DSM 962 instrument equipped with a TRACOR VOYAGER EDX apparatus. Prior to analysis the samples, embedded in resin, were covered with a very thin carbon film to become conductive.
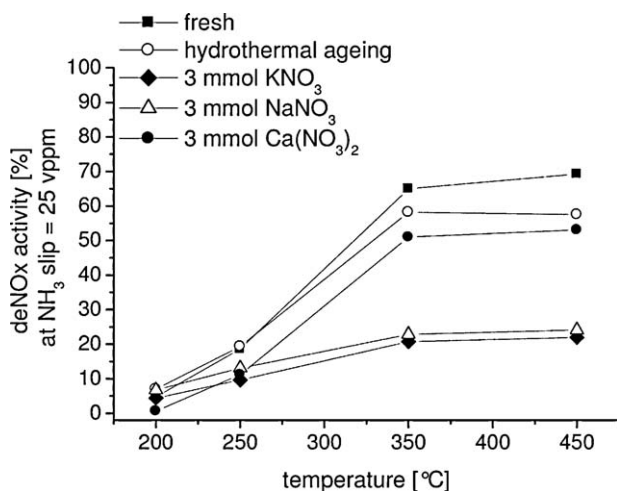
DRIFTS investigations were performed with a FTIR spectrometer Equinox55 (Bruker Optics). Prior to ammonia adsorption the samples were dried at 200 °C under a N$_2$ flow. Afterwards the samples were saturated with NH$_3$ (1038 ppm NH$_3$, N$_2$) at 50 °C for 15 min. DRIFT spectra were collected before and after saturation with NH$_3$.
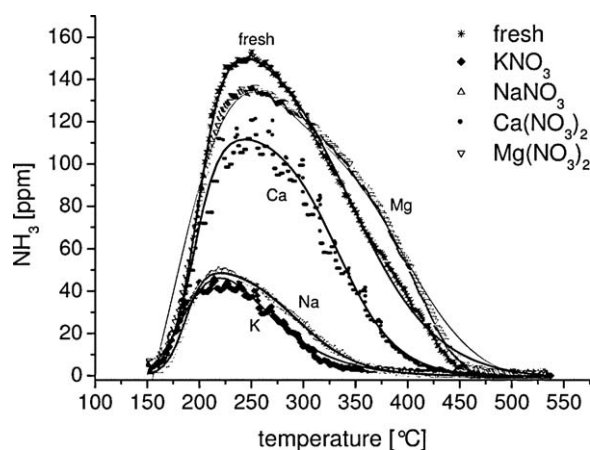
3. Results and discussion

3.1. Poisoning effect of single components

3.1.1. Effect of alkaline and alkaline earth metals

Alkaline as well as alkaline earth metals are strong poisons to the V$_2$O$_5$ based SCR catalyst. These effects were observed at poisoning of the catalysts via liquid-phase (i.e., impregnation, Fig. 1) and gas-phase procedure (i.e., aerosol, Fig. 2).

Fig. 2. DeNOx activity as a function of temperature of fresh, hydrothermal aged and K, Na and Ca (with a molar throughput of 3 mmol) poisoned catalysts; conditions: 1000 vppm NO, 1000 vppm CO, 5 vol.% CO$_2$, 8 vol.% O$_2$, 5 vol.% H$_2$O and balance N$_2$ at NH$_3$ slip of 25 vppm and 50,000 h^{-1}; poisoning of 400 cpsi monoliths by aerosols.

The deactivating effect of alkaline and alkaline earth metals increases in the order K > Na > Ca > Mg, as shown in Fig. 1 for impregnated monolithic catalysts. At a theoretical loading of the poison of 0.25 mmol/g washcoat an almost complete catalyst deactivation can be observed in case of poisoning with potassium and sodium. Calcium and especially magnesium lead to a weaker deactivating effect. This is attributed to the basicity of these additives, which is related to the intensity of poisoning. Alkaline (and probably alkaline earth) metals oxides increase the required energy for proton abstraction of the V–OH groups and cause a decrease of Brønsted acidity of the catalyst [15]. But Brønsted acid sites are responsible for adsorption of ammonia which reacts with gaseous or weakly adsorbed NO [4]. A lower ammonia adsorption capacity after poisoning was shown using ammonia TPD measurements (Fig. 3). Hereby, catalyst powders were impregnated with 0.3 mmol poison/g catalyst. An addition of potassium lead to a fivefold drop of the adsorbed ammonia amount compared to the fresh catalyst (Table 1). At the same time, an increased amount of ammonia chemisorbed by the catalyst was observed which corresponds to a decreased basicity of poisons in the order Mg > Ca > Na > K.

These results were confirmed when the catalysts were poisoned with aerosols containing 3 mmol poison in each case. The precursors were decomposed thermally and fed through the monolithic catalyst in form of inorganic particulates. The amount of poisons adsorbed by the catalysts after a poisoning time of 50 h is shown in Table 2. For a comparable amount of the adsorbed poison, an identical order in the strength of deactivation was observed, i.e. K > Na ≫ Ca which is equal to impregnated catalysts. As presented above, the catalytic performance of V$_2$O$_5$ based catalysts is strongly dependent on the amount of adsorbed ammonia and, thus, on the relative surface coverage of the catalyst. However, this does not refer to magnesia. The NH$_3$ surface coverage is a function of the ammonia concentration in the feed for which reason a strong dependence of

Table 1
NH$_3$-TPD results of fresh and poisoned catalysts.

Catalyst/poisoning component	Adsorbed NH$_3$ amount [mL/g]
Fresh	1.9 ± 0.1
K	0.4
Na	0.5
Mg	2.2
Ca	1.5
Ca/P	1.7
Ca/S	2.1

Table 2
Poison loading of catalysts and % of throughput after poisoning by aerosols.

Poisoning component	Poisoning method	Content [wt.%] (washcoat)	% of throughput
3 mmol Ca(NO₃)₂	Aerosol	Ca: 0.26	7
3 mmol KNO₃	Aerosol	K: 0.27	7
3 mmol NaNO₃	Aerosol	Na: 0.2	9
3 mmol (NH₄)₂HPO₄	Aerosol	P: 0.2	7
11 mmol (NH₄)₂HPO₄	Aerosol	P: 3.9	36

the catalytic activity from the NH_3/NO ratio is assumed. The low amount of Ca was able to marginally reduce the ammonia adsorption capacity so that at a deNOx activity, comparable to a fresh catalyst, a slightly higher ammonia slip was observed. This result, in a more drastic extent, was also found in the case of a serial catalyst (400 cpsi) doped with potassium by the impregnation procedure. Hereby, a potassium content of 0.3 mmol/g washcoat was chosen. This catalyst was strongly deactivated, modest activities (4%) were evident only at high ammonia slips (1100 vppm) indicating considerable reduction of ammonia surface coverage (not shown). Decreased ammonia amounts as well as strong deactivation of catalysts with 0.3 mmol potassium/g were already shown in Figs. 1 and 3.

DRIFTS experiments also confirm a reduction of the ammonia adsorption capacity of catalysts poisoned with 0.3 mmol Ca/g catalyst by using catalyst powders. Fig. 4 shows the spectra of fresh catalysts and those doped with Ca before and after saturation with ammonia in a range of 3800–1200 cm^{-1}. The signals at 1425 cm^{-1} and 1670 cm^{-1} result from the asymmetric and symmetric deformation mode of NH_4^+ adsorbed on Brønsted acid sites [25]. The signals in the range from 2400 cm^{-1} to 3500 cm^{-1} are attributed to weakly adsorbed ammonia whereas coordinated ammonia exhibits a signal at 1605 cm^{-1} [25]. It can be observed that less ammonia is adsorbed on the poisoned catalyst. Additional, after saturation with ammonia a decrease in signal intensity around 1998 cm^{-1} due to the first overtone vibration of $V^{5+}=O$ [25] is observed. According to Topsøe et al. [4] these sites are relevant because they activate ammonia which is adsorbed on Brønsted acid sites. This activation is a requirement for the reaction of the bonded ammonia species with gaseous NO [4].

3.1.2. Poisoning effect of phosphates

The poisoning of the catalysts with phosphorus was conducted by impregnation with an ammonium hydrogen phosphate solution as well as by aerosols, generated by injecting a dilute solution of ammonium hydrogen phosphate in the apparatus. The poisoning with the ammonium salts lead to gaseous components like NH_3 and orthophosphoric acid which comes close to decomposition products
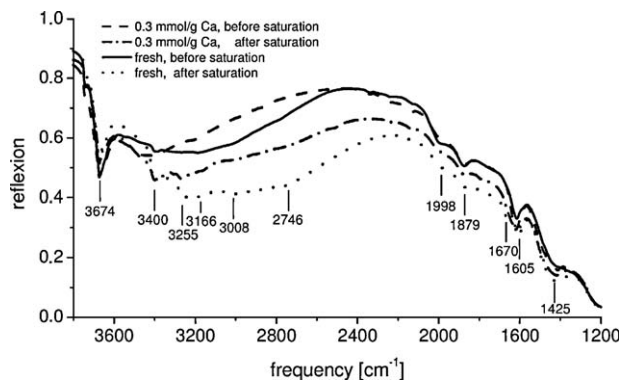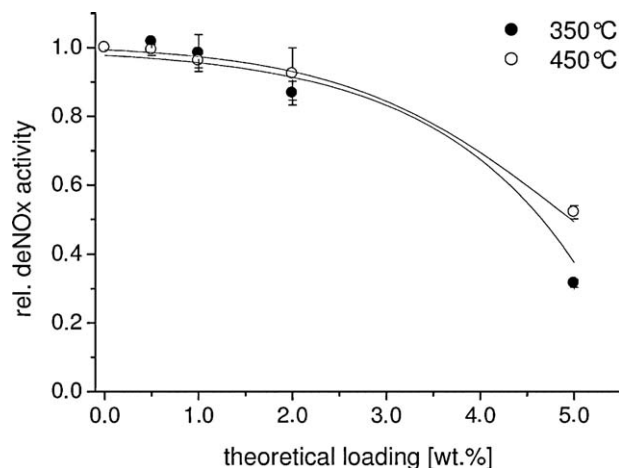
Fig. 5. Relative deNOx activity as a function of P loading; conditions: 1000 vppm NO, 1000 vppm NH₃, 1000 vppm CO, 5 vol.% CO₂, 8 vol.% O₂, 5 vol.% H₂O and balance N₂ at 350 °C/450 °C and 50,000 h⁻¹; poisoning of 72 cpsi monoliths by impregnation.

delivered through the catalytic SCR system. Both approaches lead to a deactivation when high amounts of phosphorus were used. Doping by impregnation results in a poisoning effect if a phosphorus amount of 2 wt.% is exceeded (Fig. 5). Similar observations were made when catalysts were poisoned via the gas phase. A molar throughput of 11 mmol P causes a strong deactivation. This catalyst adsorbed 36% of the total phosphorus amount which corresponds to 3.9 wt.% based on the amount of the catalyst washcoat. The poisoned catalyst shows a deNOx activity of 21% at an ammonia slip of 25 vppm, the hydrothermal aged catalyst exhibits an activity of 58%. A molar throughput of 3 mmol P leads to an activity comparable to the hydrothermal aged catalyst (Fig. 6). This catalyst shows a phosphorus loading of just 0.2 wt.%. Hereby, the accumulation of phosphorus is probably limited by the hydrolysis of the phosphorus deposits since H₂O is a component of the aerosol and the feed under SCR reaction conditions [8]. At a low phosphorus concentration in the aerosol the hydrolysis becomes more important, particularly at low deposition rates as in the case of a phosphorus throughput of 3 mmol, whereas at higher concentrations (phosphorus throughput of 11 mmol) the deposition rates of the particles are more relevant [8].

It is believed that formation of polyphosphates takes place when a certain phosphorus concentration at the catalyst surface is exceeded. Following aspects support this statement: NH_3-TPD experiments of a fresh sample as well as one with a phosphorus
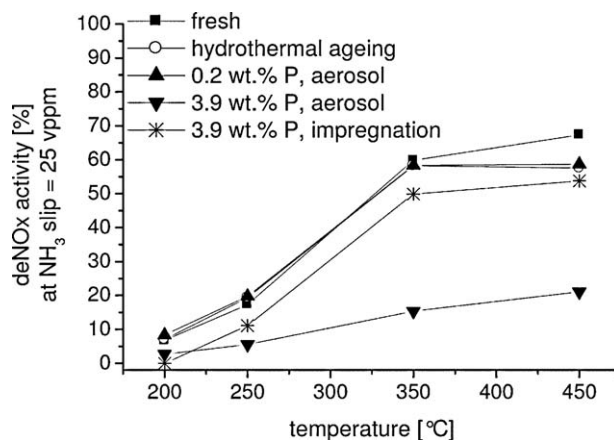

Fig. 4. DRIFT spectra of fresh and with Ca doped catalyst before and after saturation with ammonia at 50 °C in a frequency range 3800–1200 cm^{-1}; poisoning of powders by impregnation.


Fig. 6. DeNOx activity as a function of temperature of fresh, hydrothermal aged and P (poisoning by aerosols, molar throughput of 3 and 11 mmol; poisoning by impregnation) poisoned catalysts; 1000 vppm NO, 1000 vppm CO, 5 vol.% CO₂, 8 vol.% O₂, 5 vol.% H₂O and balance N₂ at NH₃ slip of 25 vppm and 50,000 h⁻¹.
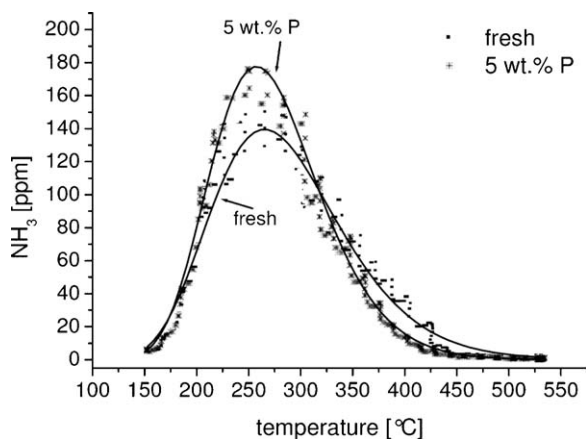
Fig. 7. NH$_3$-TPD curve of fresh and P (5 wt.%) poisoned catalysts. NH$_3$ adsorption temperature: 50 °C, temperature ramp: 10 K/min; poisoning of powders by impregnation.

concentration of 5 wt.% show an increased amount of adsorbed NH$_3$ with higher phosphorus loading (Fig. 7). These results are attributed to an increased acidity of the catalyst surface with higher phosphorus concentration due to a preferred formation of surface phosphates. At the same time, these groups reduce the specific BET surface area of the catalysts. After depositing 122 mg P (3.9 wt.% P) via the aerosol technique a decrease of the specific BET surface area from 34 m^2/g (for the non-modified, hydrothermal aged sample) to 20 m^2/g was observed, probably due to glassy phosphorus containing layers. The coverage of the catalyst surface is already known as a deactivating mechanism [8,9]. On the contrary, the specific BET surface area of the catalyst with a low phosphorus loading of 0.2 wt.% (6 mg) is not affected. XPS experiments also show coverage of the catalyst surface (Fig. 8) because the V 2p signal at a binding energy of 516 eV, which can be clearly seen for the fresh sample, disappeared at high phosphorus loading of 3.9 wt.%. These results indicate that the active vanadium sites are present under a
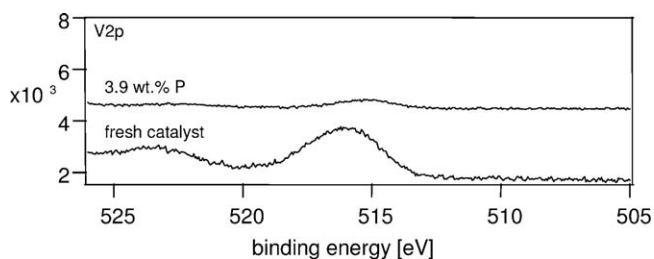
Fig. 8. XPS spectra of fresh and P poisoned catalyst; poisoning of 400 cpsi monolith by aerosol, molar throughput of 11 mmol P (3.9 wt.% P).
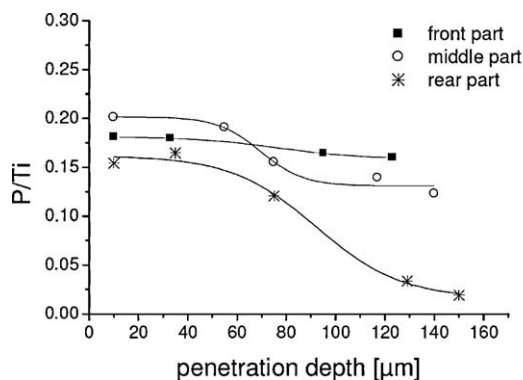
phosphorus containing layer and, thus, they cannot take place in the SCR reaction. Similar effects could be seen in case of the other catalyst compounds like W and Ti (not shown).

To compare the chosen approaches of poisoning, an 400 cpsi segment, typically used for poisoning by inorganic particulate, was now impregnated and tested under the same SCR conditions, adjusting a phosphorus amount of 3.9 wt.%. This catalyst, doped by impregnation, shows a level of activity which is comparable to the hydrothermal aged catalyst (Fig. 6). However, poisoning by an aerosols leads to a strong deactivation.

Although both catalysts show the same loading with poison (3.9 wt.%) a big difference in catalytic performance was observed. Differences in distribution of phosphorus were investigated with REM/EDX experiments. For this analysis three parts of the catalyst were selected, based on increasing flow direction, and the distribution of poison in radial direction was determined. As an indicator the P/Ti ratio, latter represents a main component of the catalyst washcoat, was chosen. High amounts of phosphorus were found in the front and in the middle part in the complete thickness of the catalyst washcoat poisoned by an aerosol (Fig. 9, left). Mobile particles deposited on the catalyst surface can be sucked into the catalyst layer by capillary forces. The rear part shows comparable poison amounts only in low penetration depths. In the case of impregnation, the catalyst shows almost an uniform distribution of phosphorus in all three different parts of the catalyst (Fig. 9, right). Hereby, catalyst pores are filled with solution by capillary forces which lead to a distribution of the solution into the pore structure.

From Table 3 it can be concluded that the strong reduced activity of the catalyst, poisoned by the aerosol technique, is due to a strong reduced specific BET surface area. The textural parameters show a lower catalyst pore volume and an increased average pore diameter. REM/EDX analyses confirm these results, high phosphorus concentration is obvious in the almost complete catalyst. On the contrary, the catalyst modified by impregnation shows average pore diameter and pore volume comparable to the hydrothermal aged catalyst. This agrees with REM/EDX analysis which shows lower phosphorus concentration on and in the catalytic washcoat and an uniform distribution. This concentration is too low to influence the morphology as well as the performance of the catalyst in a drastic extent.

3.1.3. Poisoning by transition metals

For poisoning by transition metals chromium and copper were chosen. These components reduce the deNOx activity as can be seen in Fig. 10 for impregnated catalysts. The slightly lower activity of poisoned catalysts is attributed to an increased production of N$_2$O with higher temperature and poison loading so that at a maximum concentration of 2 wt.% of Cr and Cu a relative deNOx activity of 0.79 and 0.82, respectively, is observed. An almost
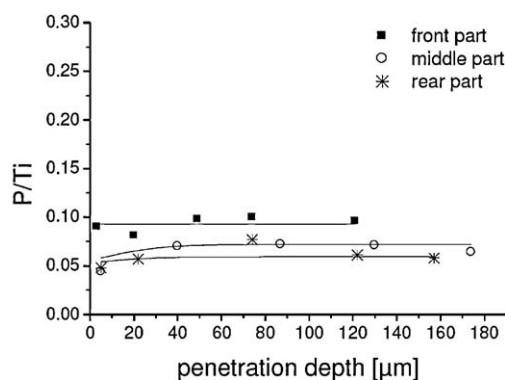

Fig. 9. P/Ti ratio as function of penetration depths of phosphorus of an aerosol poisoned (left) and an impregnated (right) catalyst with a phosphorus loading of 3.9 wt.%.

Table 3
Textural properties of the hydrothermal aged and with phosphorus poisoned catalyst.

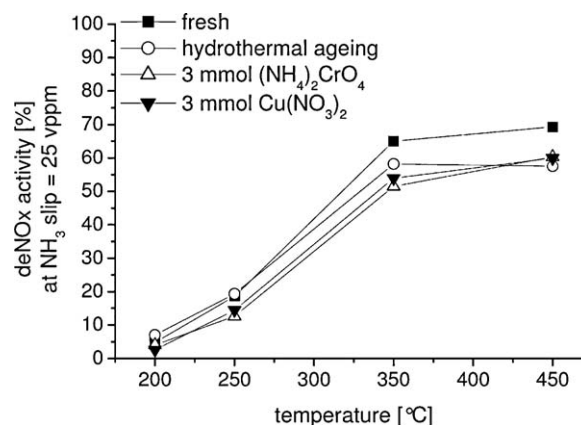| Catalyst/poisoning component	Poisoning method	Content [wt.%] (washcoat)	BET surface area [m^2/g]	Average pore volume [cm^3/g]	Average pore diameter [nm]
Hydrothermal aged	–	–	34	0.13	15
$(NH_4)_2HPO_4$	Aerosol	P: 3.9	20	0.09	17
$(NH_4)_2HPO_4$	Impregnation	P: 3.9	39	0.12	12
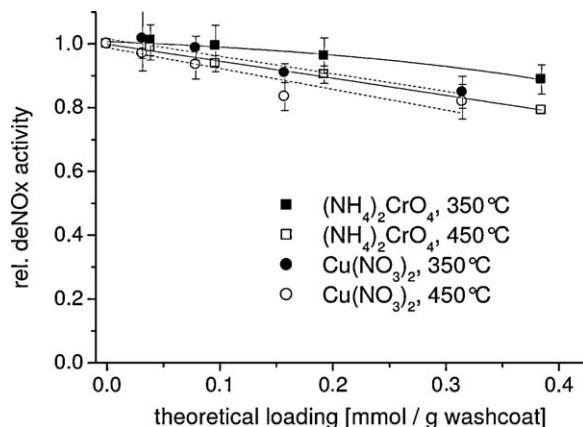
Fig. 10. Relative deNOx activity as a function of Cr and Cu loading; conditions: 1000 vppm NO, 1000 vppm NH$_3$, 1000 vppm CO, 5 vol.% CO$_2$, 8 vol.% O$_2$, 5 vol.% H$_2$O and balance N$_2$ at 350 °C/450 °C and 50,000 h^{-1}; poisoning of 72 cpsi monoliths by impregnation.

complete conversion of NO at 450 °C (not shown) indicates that no additional limitation of mass transport by high amounts of poisons occurs. Simultaneously, N$_2$ selectivity decreases with higher poison amount to a stronger extent when the catalyst was modified by Cr instead of Cu. Hereby a N$_2$O selectivity of 18% and 10% at 450 °C for Cr and Cu poisoned catalysts were detected. These correspond to N$_2$O amounts of 154 and 76 vppm as presented in Table 4.

The poisoning by inorganic particulate was carried out with a molar throughput of 3 mmol Cr and Cu. This approach which involves the thermal decomposition of the precursors seems to be more realistic, the constituents are inserted into the catalytic

Table 4
Activity and selectivity data of fresh and Cr and Cu poisoned catalyst; poisoning of 72 cpsi monoliths by impregnation.

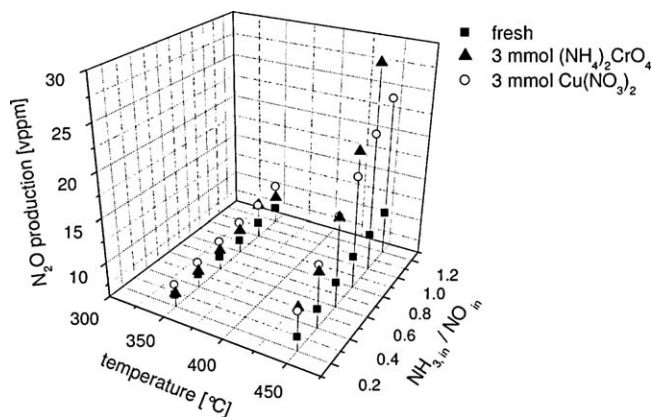| Catalyst	T [°C]	Rel. deNOx	$S(N_2O)$ [%]	N$_2$O [vppm]
Fresh	350	–	1	8 ± 1
0.2 wt.% Cr	350	1.01 ± 0.05	1	9 ± 1
0.5 wt.% Cr	350	0.99 ± 0.06	1	9 ± 2
1 wt.% Cr	350	0.96 ± 0.06	2	11 ± 2
2 wt.% Cr	350	0.89 ± 0.05	4	24 ± 5
0.2 wt.% Cu	350	1.06 ± 0.23	2	12 ± 3
0.5 wt.% Cu	350	0.99 ± 0.04	3 ± 1	20 ± 6
1 wt.% Cu	350	0.91 ± 0.03	5 ± 1	28 ± 7
2 wt.% Cu	350	0.85 ± 0.05	6 ± 1	34 ± 3
Fresh	450	–	1	11 ± 1
0.2 wt.% Cr	450	0.99 ± 0.03	2	14 ± 1
0.5 wt.% Cr	450	0.94 ± 0.03	4 ± 1	32 ± 7
1 wt.% Cr	450	0.90 ± 0.02	7 ± 1	61 ± 8
2 wt.% Cr	450	0.79	18	154
0.2 wt.% Cu	450	0.97 ± 0.02	3	25 ± 2
0.5 wt.% Cu	450	0.94 ± 0.04	6 ± 2	53 ± 13
1 wt.% Cu	450	0.83 ± 0.04	10 ± 1	74 ± 2
2 wt.% Cu	450	0.82 ± 0.05	10	76 ± 2

aftertreatment system by abrasion of the engine. The catalyst poisoned by Cr or Cu adsorbed 7% and 0.7% of the total poison amount which corresponds to 0.36 wt.% Cr and 0.04 wt.% Cu, respectively, in relation to the washcoat. These concentrations affect the catalytic activity as well as the ammonia slip in a marginal scale for high values of α, i.e. the ratio NH$_{3,in}$/NO$_{in}$ (not shown). For a better overview, catalytic performance is shown at an ammonia slip of 25 vppm (Fig. 11) which is close to mobile applications. In this case the catalysts show comparable activities to the hydrothermal aged catalyst.

In spite of the low poison amount adsorbed by the catalysts, particularly in case of copper, the production of N$_2$O was detected. Hereby the N$_2$O amount is dependent on the temperature as well as on the ammonia concentration in the feed (Fig. 12). A higher ammonia concentration and temperature lead to an increased N$_2$O formation due to ammonia oxidation. The formed N$_2$O amount

Fig. 11. DeNOx activity as a function of temperature of fresh, hydrothermal aged and Cr and Cu poisoned catalysts; conditions: 1000 vppm NO, 1000 vppm CO, 5 vol.% CO$_2$, 8 vol.% O$_2$, 5 vol.% H$_2$O and balance N$_2$ at NH$_3$ slip of 25 vppm and 50,000 h^{-1}; poisoning of 400 cpsi monoliths by aerosols.

Fig. 12. N$_2$O production as a function of temperature and NH$_{3,in}$/NO$_{in}$ ratio; conditions: 1000 vppm NO, 1000 vppm CO, 5 vol.% CO$_2$, 8 vol.% O$_2$, 5 vol.% H$_2$O and balance N$_2$ at NH$_{3,in}$/NO$_{in}$ = 0.2–1.2, 50,000 h^{-1} and 350 °C/450 °C; poisoning of 400 cpsi monoliths by aerosols.

with a maximum of 30 vppm corresponds to a N_2O selectivity of 3%. The lower values compared to the selectivities obtained after poisoning by impregnation (Table 4) are attributed to a much lower Cr and Cu loading on the catalyst after poisoning with inorganic particulate. Comparisons of N_2O selectivities of the impregnated catalysts with a low poison amount also show marginal ammonia oxidation.

3.2. Poisoning effects in multicomponent systems

To identify interactions of poisons and to clarify modes of action, measurements of SCR activity and N_2O formation were carried out in a 6 component system combining different poisons.

Six components (factors) were chosen to construct a model using the identified catalyst poisons K, Ca, Zn and phosphate as well as Cu which leads to an increased production of N_2O, and sulphate. Inorganic poisons were introduced by impregnation, varying the amounts of poisons over five concentration levels (0, 0.07, 0.1, 0.13, 0.2 mmol/g washcoat).

The number of single experiments of a fractional experimental plan would result in 15,625 (=level^{factors}) experiments at each temperature. To overcome this enormous amount of experiments Design of Experiments (DOE) was applied. It allows the identification of interactions of parameters with preferably few experiments. The experimental designs were made by a Response Surface Method applying a D-optimal design with 128 points. These points were chosen by using an algorithm. The minimal numbers of points were proposed which are dependent on the number of factors (poisons) and the coefficients of the model. The poison concentrations were converted to −1 for 0 mmol/g washcoat and +1 for 0.2 mmol/g washcoat.

At first, we started with three concentration levels and used an experimental plan for analysis with a quadratic model to diminish the required number of experiments. For this purpose the concentration levels of (0, 0.1, and 0.2) mmol/g washcoat were used. Afterwards, an experimental plan for analysis with a cubic model was applied. In this model 83 possible interactions were included, which consider the effects of single factors (poisons) as well as interactions of two and three factors (poisons):

$$\text{deNOx }[\%] = \text{deNOx}_{fresh} + \sum_i a_i \cdot c_i^{x_i} + \sum_{i,j} a_{ij} \cdot c_i^{x_i} \cdot c_j^{x_j}$$
$$+ \sum_{i,j,k} a_{ijk} \cdot c_i \cdot c_j \cdot c_k \quad x = 1, 2$$

Table 5
Model for deNOx activity at 350 °C.

350 °C, deNOx$_{fresh}$ = 53%		
deNOx [%] = deNOx$_{fresh}$ + $\sum_i a_i \cdot c_i^{x_i}$ + $\sum_{i,j} a_{ij} \cdot c_i^{x_i} \cdot c_j^{x_j}$ + $\sum_{i,j,k} a_{ijk} \cdot c_i \cdot c_j \cdot c_k$ $x = 1, 2$		
Effect $c_i^{x_i}$, $c_i^{x_i} * c_j^{x_j}$, $c_i^{x_i} * c_j^{x_j} * c_k^{x_k}$		a_i, a_{ij}, a_{ijk}
0–0.2 mmol/g	$P > F$	deNOx [%]
*K	<0.0001	−107.6
*Ca	<0.0001	−45.6
*Zn	0.0003	−13.3
*P[a]	0.2807	104.3
*S	<0.0001	25.1
*K × Ca	0.0231	36.3
*K × P	0.0020	−122.9
*K × S	0.0708	195.2
*Ca × P[a]	0.3619	−584.6
*Ca × S	0.0035	239.4
*P^2	0.0388	−423.4
*K × Ca × S	0.0034	−1260.4
*Ca × P^2	0.0038	2745.0
Intercept		52.3

[a] Term not significant.

Table 6
Model for N_2O production at 450 °C.

| 450 °C, N_2O_{fresh} = 10 vppm		
N_2O [vppm] = N_2O_{fresh} + $\sum_i a_i \cdot c_i^{x_i}$ + $\sum_{i,j} a_{ij} \cdot c_i^{x_i} \cdot c_j^{x_j}$ + $\sum_{i,j,k} a_{ijk} \cdot c_i \cdot c_j \cdot c_k$ $x = 1, 2$		
Effect $c_i^{x_i}$, $c_i^{x_i} * c_j^{x_j}$, $c_i^{x_i} * c_j^{x_j} * c_k^{x_k}$		a_i, a_{ij}, a_{ijk}
0–0.2 mmol/g	$P > F$	N_2O [vppm]
*K	<0.0001	−7.4
*Ca	0.0007	6.4
*Cu	<0.0001	177.1
*P	<0.0001	−3.4
*S	<0.0001	−6.9
*K × Ca	0.0320	−51.7
*K × Cu	<0.0001	−387.1
*K × P	0.0282	52.8
*K × S	0.0005	83.8
*Ca × Cu	0.0004	−88.0
*Cu × P	<0.0001	−169.8
*Cu × S	<0.0001	109.5
Intercept		10.0

Relevant effects were identified by comparison of variance of the sample test towards the average variance of repetition experiments (F-test). A certain identification of an effect is given when P (probability) > F: <0.05. In this case there is a probability
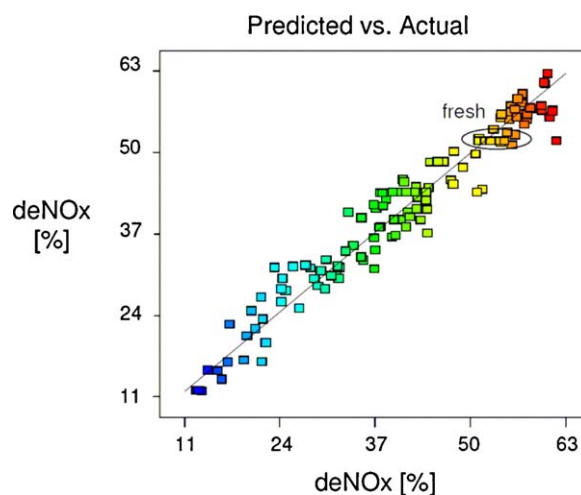
Fig. 13. Prediction of the model for deNOx activity at 350 °C; conditions: 1000 vppm NO, 1000 vppm NH_3, 1000 vppm CO, 5 vol.% CO_2, 8 vol.% O_2, 5 vol.% H_2O and balance N_2 at 50,000 h^{-1}; poisoning of 72 cpsi monoliths by impregnation.
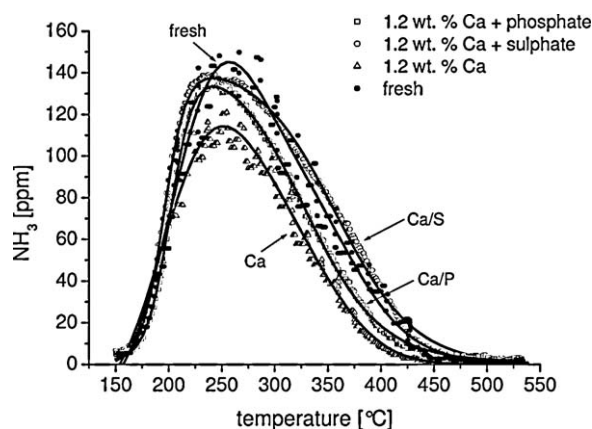
Fig. 14. NH_3-TPD curve of fresh, Ca, Ca/P and Ca/S poisoned catalysts. NH_3 adsorption temperature: 50 °C, temperature ramp: 10 K/min; poisoning of powders by impregnation.
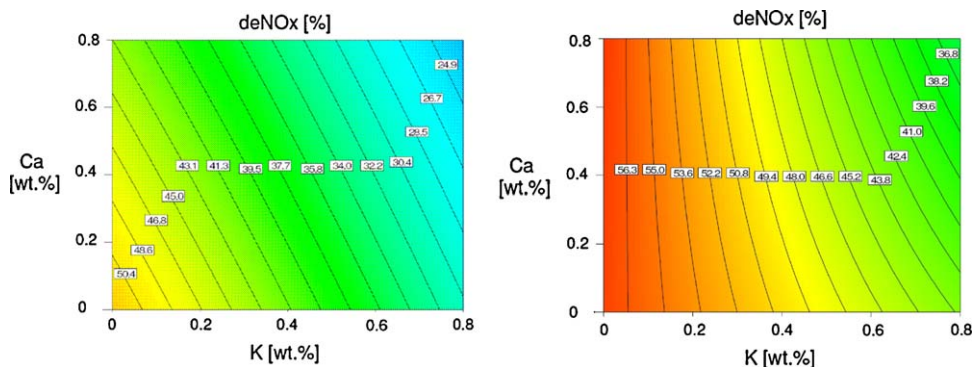
Fig. 15. Illustration of deNOx activity as a function of Ca and K loading at 350 °C without (left) and with an addition (right) of sulphates; conditions: 1000 vppm NO, 1000 vppm NH_3, 1000 vppm CO, 5 vol.% CO_2, 8 vol.% O_2, 5 vol.% H_2O and balance N_2 at 50,000 h^{-1}; poisoning of 72 cpsi monoliths by impregnation.

of 95% that the effect do exist. No significant effect is described at $P > F$: > 0.1. The effects on SCR activity and N_2O formation were determined with the equations in Tables 5 and 6 using corresponding concentrations and coefficients. A cubic model for deNOx activity in a multicomponent system at a temperature of 350 °C is given in Table 5. A model gained at 250 °C is not presented due to a low activity of the fresh catalyst. In this case, an unfavourable signal to noise relation may lead to a few incorrect data which result in a erroneous identification of an effect. Fig. 13 indicates that the gained model for deNOx activity at 350 °C shows a very good correlation with the experimental data. Moreover, the fresh catalysts (8 per each monolith) show comparable activities. Therefore, this model can be used to predict the effects and the interactions of catalyst poisons in combination.

The model confirms our previous results which show a strong deactivating effect of potassium and calcium. The combination of calcium or (potassium) with phosphate or sulphate leads to an alleviated poisoning due to a regeneration of the ammonia adsorption capacity of the catalyst as shown by NH_3-TPD experiments (Fig. 14). A strong influence on catalytic performance of a second doping element in the presence of calcium was already observed due to an increased ammonia adsorption constant [26]. The regeneration of ammonia adsorption capacity and, consequently, a higher ammonia surface coverage is attributed to formation of corresponding phosphates and sulphates which (i) are also able to adsorb ammonia due to an increased Brønsted acidity [15] and (ii) prevent interaction of calcium with active sites as it can be deduced from the increased amount of adsorbed ammonia in case of the phosphates and sulphates containing samples compared to the catalyst poisoned only by Ca (Table 1).

A different illustration of the regeneration of the ammonia adsorption capacity and, thus, a higher activity of the calcium and potassium poisoned catalyst in the presence of sulphates can also be seen in Fig. 15. Hereby, the activities are presented with and without an addition of sulphates (0.2 mmol/g washcoat). A strong deactivation is observed if there is not any sulphate present; the catalyst reached just 25% of deNOx activity at a combination of 0.2 mmol Ca and K per gram of washcoat. The addition of sulphates leads to an increase in activity of 12%. Moreover, a higher activity compared to a fresh catalyst (53%) is observed even in the presence of K and higher amounts of Ca in combination with sulphates.

Furthermore, the model shows no strong effect of phosphorus in the investigated concentration range. At a maximum phosphorus concentration of 0.2 mmol/g washcoat, a deNOx activity of 56% is observed. This is in agreement with the experimental results described above. The observed deactivation by phosphorus was attributed to its high amounts which led to a decrease of the specific BET surface area and the coverage of active sites due to phosphates on the catalytic surface. The concentration of

phosphorus used in the multicomponent systems with a maximum amount of 0.6 wt.% is too low to deactivate the catalyst.

In addition, the model shows a deactivating effect of zinc but none of copper. Therefore, the latter is not listed in Table 5. This is not surprising because copper does not exhibit a strong influence on the catalytic activity in a concentration range of 0–0.2 mmol/g washcoat as shown in Fig. 10.

A prediction of a model was also conducted for the production of the greenhouse gas N_2O (Table 6) at 450 °C. This can be described with a 2FI model with satisfying accuracy.

High N_2O amounts were detected at poisoning with copper, as already shown, but this effect is strongly reduced by adding copper in combination with alkaline (and alkaline earth) metals. These results go along with a decreased deNOx activity. This is not surprising because both the formation of N_2O and the selective catalytic reduction of NO with NH_3 assume the adsorption of ammonia on Brønsted acid sites. Poisoning with alkaline metals leads to a reduced ammonia adsorption capacity and, thus, to a decreased production of N_2O and deNOx activity. Zn has no effect on the formed N_2O amount, and hence is not listed in Table 6.

4. Conclusions

The poisoning effects of inorganic components to a V_2O_5/WO_3–TiO_2 catalyst have been investigated using different approaches for catalyst modification, i.e. impregnation procedure as well as poisoning by inorganic particulate.

Doping with alkaline and alkaline earth metals result in a strong catalyst deactivation due to a reduced ammonia storage capacity. This is already obvious at low poison concentration. Hereby the poisoning effect of the additives is related to the basicity and increases in the order K > Na > Ca > Mg. Phosphate is a further strong deactivating component. In this case an activity loss is only observed when a critical phosphorus concentration on the catalyst surface is exceeded. Moreover, it was possible to show that phosphorus compounds, formed on the catalyst surface, increases the acidity of the catalyst. Simultaneously, the formation of phosphates results in a decreased catalytic surface due to pore blocking. Hereby, an impregnation procedure seems to be less harmful compared to poisoning by aerosols. Impregnation leads to an uniform phosphorus distribution in the washcoat while in the case of poisoning by aerosols high amounts of poison were found in the outer washcoat region.

The investigation of the poisoning effect of different element combinations using Design of Experiments (DOE) exhibit an alleviated poisoning of Ca in the presence of phosphates and sulphates due to a regeneration of the ammonia adsorption capacity of the catalyst. The phosphate and sulphate species are

able to adsorb ammonia and to prevent the interaction of calcium with active sites of the catalyst.

Transition metals like chromium and copper are moderate poisoning components but they lead to a reduction of the N_2 selectivity related to formation of N_2O. High concentrations (2 wt.%) of these components lead to N_2O selectivities of 10% (with Cu) and 18% (with Cr). Furthermore, this effect was not detected by a simultaneous poisoning of the catalyst with copper in combination with strong deactivating components like alkaline metals due to a reduced ammonia adsorption capacity caused by the latter.

Acknowledgments

References

[1] H. Bosch, F. Janssen, Catal. Today 2 (1988) 369–532.
[2] P. Forzatti, Catal. Today 62 (2000) 51–65.
[3] J.P. Chen, R.T. Yang, Appl. Catal. A: Gen. 80 (1992) 135–148.
[4] N.-Y. Topsøe, J.A. Dumesic, H. Tapsøe, J. Catal. 151 (1995) 241–252.
[5] S. Soyer, A. Uzun, S. Senkan, I. Onal, Catal. Today 118 (2006) 268–278.
[6] M. Anstrom, N.-Y. Topsøe, J.A. Dumesic, J. Catal. 213 (2003) 115–125.
[7] J. Beck, J. Brandenstein, S. Unterberger, K.R.G. Hein, Appl. Catal. B: Environ. 49 (2004) 15–25.
[8] F. Castellino, S.B. Rasmussen, A.D. Jensen, J.E. Johnsson, R. Fehrmann, Appl. Catal. B: Environ. 83 (2008) 110–122.
[9] J. Blanco, P. Avila, C. Barthelemy, A. Bahamonde, J.A. Odriozola, J.F. Garcia de la Banda, H. Heinemann, Appl. Catal. 55 (1989) 151–164.
[10] J.P. Chen, M.A. Buzanowski, R.T. Yang, J.E. Cichanowicz, J. Air Waste Manage. Assoc. 40 (1990) 1403–1409.
[11] H. Kamata, K. Takahashi, C.U. Ingemar Odenbrand, J. Mol. Catal. A: Chem. 139 (1999) 189–198.
[12] L. Lisi, G. Lasorella, S. Malloggi, G. Russo, Appl. Catal. B: Environ. 50 (2004) 251–258.
[13] Å. Kling, C. Andersson, Å. Myringer, D. Eskilsson, S.G. Järås, Appl. Catal. B: Environ. 69 (2007) 240–251.
[14] Y. Zheng, A.D. Jensen, J.E. Johnsson, J.R. Thøgersen, Appl. Catal. B: Environ. 83 (2008) 186–194.
[15] J.P. Chen, R.T. Yang, J. Catal. 125 (1990) 411–420.
[16] A.L. Kustov, S.B. Rasmussen, R. Fehrmann, P. Simonsen, Appl. Catal. B: Environ. 76 (2007) 9–14.
[17] F. Moradi, J. Brandin, M. Sohrabi, M. Faghihi, M. Sanati, Appl. Catal. B: Environ. 46 (2003) 65–76.
[18] Y. Zheng, A.D. Jensen, J.E. Johnsson, Appl. Catal. B: Environ. 60 (2005) 253–264.
[19] M. López Granados, C. Larese, F. Cabello Galisteo, R. Mariscal, J.L.G. Fierro, R. Fernández-Ruíz, R. Sanguino, M. Luna, Catal. Today 107–108 (2005) 77–85.
[20] C. Larese, F. Cabello Galisteo, M. López Granados, R. Mariscal, J.L.G. Fierro, M. Furió, R. Fernández-Ruiz, Appl. Catal. B: Environ. 40 (2003) 305–317.
[21] M.J. Rokosz, A.E. Chen, C.K. Lowe-Ma, A.V. Kucherov, D. Benson, M.C. Paputa Peck, R.W. McCabe, Appl. Catal. B: Environ. 33 (2001) 205–215.
[22] F.M. Zanon Zotin, O. Da Fonseca Martins Gomes, C.H. de Oliveira, A. Alcover Neto, M.J. Baldini Cardoso, Catal. Today 107–108 (2005) 157–167.
[23] M. Lucas, P. Claus, Appl. Catal. A: Gen. 254 (2003) 35–43.
[24] P. Kern, M. Klimczak, M. Lucas, P. Claus, Chem. Eng. Technol. 81 (2009) 289–296.
[25] D. Nicosia, I. Czekaj, O. Kröcher, Appl. Catal. B: Environ. 77 (2008) 228–236.
[26] O. Kröcher, M. Elsener, Appl. Catal. B: Environ. 77 (2008) 215–227.